Letters

A Virtual Impedance Comprehensive Control Strategy for the Controllably Inductive Power Filtering System

Yong Li, *Senior Member, IEEE*, Qianyi Liu, *Student Member, IEEE*, Sijia Hu, *Member, IEEE*, Fang Liu, *Member, IEEE*, Yijia Cao, *Senior Member, IEEE*, Longfu Luo, *Member, IEEE*, and Christian Rehtanz, *Senior Member, IEEE*

***Abstract*—In this letter, a virtual impedance comprehensive control (VICC) strategy is proposed for the controllably inductive power filtering (CIPF) system with a new filtering mechanism. This control strategy aims to satisfy the zero-impedance design precondition of the inductive power filtering system, and can dampen the harmonic resonance at the grid side. By the proposed zero-impedance control, the quality factor of the passive power device can be adjustable, and the single-tuned filter can be multituned. First, the main circuit topology for implementing the VICC-based CIPF is presented. Then, on the basis of the multipurpose control, the VICC strategy is designed. Furthermore, by means of the established equivalent circuit model and the corresponding mathematical model, the principles of the harmonic damping and the zero-impedance realization are revealed. Finally, the experimental results verify that the proposed control strategy can weaken the harmonic amplification effectively, and improve the filtering performance significantly.**

***Index Terms*—Harmonic damping, inductive power filtering (IPF), virtual impedance control, zero-impedance design.**

I. Introduction

THE traditional filtering methods mainly focus on how to improve the power quality (PQ) of the public power network [1]–[5]. However, for the PQ problems existed in the supply systems that connect the nonlinear power load with the distribution network, the filtering methods are helpless to solve the problems at the power user side efficiently [6]. Taking the rectifier transformer applied in the large-power industrial dc supply system as an example [7], [8], the traditional filters, such as the passive power filter (PPF) or the active power filter, are generally configured at the point of common coupling (PCC), and cannot reduce the harmonic currents flowing into the transformer. Hence, the harmonic components inevitably cause a series of problems to the transformer, e.g., operating loss, noise, and vibration.

In recent years, an inductive power filtering (IPF) method was proposed by Li *et al.* [9], [10]. The IPF method uses an additional zero-impedance designed winding of the converter transformer integrated with a set of single-tuned filters [9]. The harmonic magnetic potential can be balanced between the load and the additional (filtering) winding, and the harmonic leakage flux in the converter transformer can be reduced greatly. The IPF method makes the best of the filtering potential of the transformer, and not only suppress the harmonic current but also prevent it from flowing into the primary (grid) winding of the rectifier transformer, which means that the IPF method can reduce the effects of the harmonic components on the transformer. Currently, the IPF concept has been applied in the Chinese traction power supply system [11]. Literatures [12] further studied the IPF method, and proposed a topology of hybrid inductive and active filter (HIAF). The HIAF combines the advantages of IPF method with the hybrid active power filtering technology, and it makes up for the deficiency of the harmonic resonance damping. The IPF method proposed in [9] requires a necessary precondition of the dual zero-impedance design for the filtering winding and the filtering branches. Literature [13] analyzes the engineering design of the transformer winding. By adjusting the short-circuit impedances, the value of the equivalent impedance of the filtering winding might, ideally, be approximately equal to 0. However, as for the passive power device, due to the limitation of the manufacture technics, the facility budget and the existence of the line impedance, the equivalent impedance Z_{fn} of the filtering branches still exists as a nonzero resistance, while the capacitor and the inductor have been well tuned at the considered harmonic frequency. Literature [14] proposed an inductive active filtering (IAF) method. The IAF method can track the change of the nonlinear load, and the active technique is used to realize the precondition of zero-impedance design. However, it is helpless to suppress the background harmonic of the network.

Up to now, there are very few available literatures involving how to realize the essential condition of zero-impedance design of the IPF method. To solve this problem, this letter proposes a

Manuscript received June 21, 2016; revised July 19, 2016; accepted August 11, 2016. Date of publication August 17, 2016; date of current version November 11, 2016. This work was supported in part by the National Natural Science Foundation of China under Grants 51377001, 61233008, and 51520105011, in part by the International Science and Technology Cooperation Program of China under Grant 2015DFR70850, and in part by the Key S&T Special Project of Hunan Province of China under Grants 2015GK1002 and 2015RS4022. *(Corresponding authors: S. Hu and F. Liu.)*

Y. Li, Q. Liu, S. Hu, L. Luo, and Y. Cao are with the College of Electrical and Information Engineering, Hunan University, Changsha 410082, China (e-mail: yongli@hnu.edu.cn; liu7y@foxmail.com; huda_hsj@163.com; llf@hnu.edu.cn; yjcao@hnu.edu.cn).

F. Liu is with the School of Information Science and Engineering, Central South University, Changsha 410083, China (e-mail: csuliufang@csu.edu.cn).

C. Rehtanz is with the Institute of Energy Systems, Energy Efficiency and Energy Economics, TU Dortmund University, Dortmund 44227, Germany (e-mail: christian.rehtanz@tu-dortmund.de).

Color versions of one or more of the figures in this paper are available online at http://ieeexplore.ieee.org.

Digital Object Identifier 10.1109/TPEL.2016.2601086

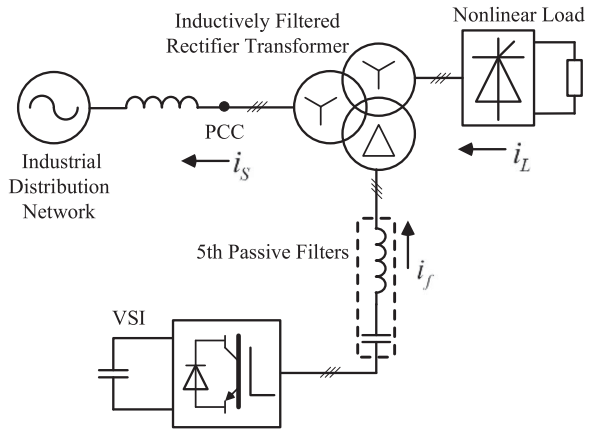

Fig. 1. Main circuit topology of the proposed CIPF system.

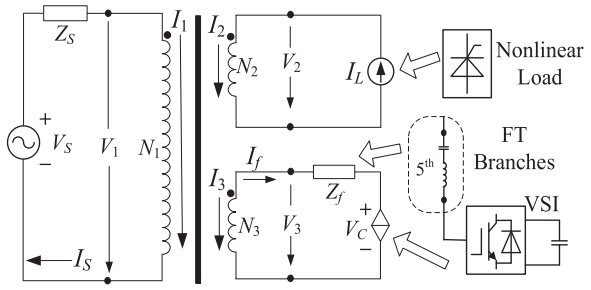

Fig. 2. Single phase wiring scheme for the CIPF system.

virtual impedance comprehensive control (VICC) strategy for the controllably inductive power filtering (CIPF) system [15], which aims to realize the zero-impedance design as required and the harmonic damping at the grid side simultaneously. The special technical features about the proposed zero-impedance control method will be revealed in theory. This letter is structured as follows. Section II describes the filtering characteristics of the CIPF system, by means of the equivalent model. In Section III, the principle of the harmonic damping control method and the zero-impedance control method are revealed, respectively. The experimental study is carried out in Section IV. Finally, the conclusion is addressed in Section V.

II. Operating Principle of the CIPF System

A. Main Circuit Topology

Fig. 1 shows the main circuit topology of the proposed VICC-based CIPF system. As the key equipment for implementing the CIPF, the inductively filtered rectifier transformer (IFRT) is installed in the vicinity of the nonlinear power load and has a three-winding structure. Its primary (grid) winding adopts the star wiring and is connected with the network. The nonlinear power load is connected with the star winding which is acted as the valve winding. The filtering winding adopts delta wiring and is connected to the fully tuned (FT) branches and the voltage-source inverter (VSI) in series. The CIPF system uses a set of single-tuned filter well tuned at fifth-order harmonic frequency as the FT branches. The proposed VICC-based CIPF system has the following technical features:

1) Based on the theory of the magnetic potential balance, the harmonic currents flowing into the valve winding and the harmonic currents induced in the filtering winding can be balanced each other. There are few harmonic currents freely flowing into the grid winding of the IFRT. Therefore, the new IFRT can mitigate the effects of the harmonic current generated by the nonlinear load on itself.
2) The VICC strategy includes the harmonic damping control and the zero-impedance control. It can weaken the impact of the background harmonic voltage on the filtering performance of the passive power device. The sensitivity of the CIPF system is far below the IPF system. Moreover, by the multipurpose control, the resistance of the filtering branches can be eliminated, and the quality factor Q of the passive filter is improved so that the design value of Q can be reached. Besides, the inverter can be controlled to be a capacitor. At the seventh-order harmonic frequency, a virtual single-tuned filter is created at the filtering branches. The VICC fully utilizes the potential of the inverter. The dependence on the manufacturing requirements of the device is reduced and the cost of the investment is saved as well.

B. Filtering Characteristics Analysis

For the thyristor-based rectifier load, the orders of the characteristic harmonic are $6k \pm 1 (k = 1, 2, 3, \ldots)$. The contents of fifth- and seventh-order harmonic currents are much higher than others. In this case, the real fifth and the virtual seventh single-tuned filter are designed. Fig. 2 shows the single-phase wiring scheme for the CIPF system. In the equivalent model, I_S, V_S, and Z_S are the grid-side current, the grid-side voltage, and the system impedance, respectively; I_L and I_f are the load current and the filtering branch current; and Z_f is the equivalent impedance of the fifth single-tuned filter. The VSI can be equivalent to a harmonic current controlled voltage source. V_C is the ac port voltage of the inverter, and can be expressed as follows:

$$V_C = K_n \cdot \sum_{n=5,7,\ldots} I_{Sn} + K_{R5} \cdot I_{f5} + K_{Z7} \angle \varphi \cdot I_{f7} \quad (1)$$

where the subscript "n" represents the harmonic component of the variables; K_n is the harmonic damping control coefficient; K_{R5} is the impurity-elimination control (IEC) coefficient; K_{Z7} is the multituned control (MTC) coefficient.

According to the theory of multiwinding transformer [16] and the principle of transformer magnetic potential balance, the following equation can be obtained to describe the impact of the load current I_{Ln} and background harmonic voltage V_{Sn} on the filtering branch current I_{fn} [9], i.e.

$$\begin{cases} I_{fn} = \dfrac{k_{21}k_{31}(Z_{1n} + Z_{Sn}) + k_{21}K_n}{(Z_{3n} + Z_{fn}) + k_{31}^2(Z_{1n} + Z_{Sn}) + k_{31}K_n} I_{Ln} \\ I_{fn} = \dfrac{k_{31}}{(Z_{3n} + Z_{fn}) + k_{31}^2(Z_{1n} + Z_{Sn}) + k_{31}K_n} V_{Sn}. \end{cases} \quad (2)$$

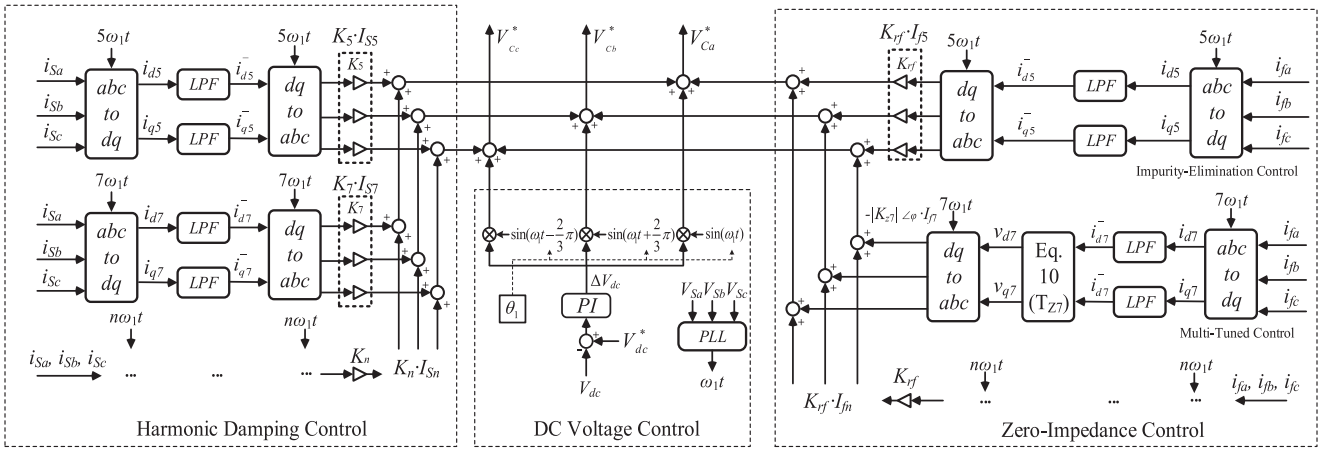

Fig. 3. Block diagram of the VICC strategy.

From (2), it can be found that the filtering performance is mainly affected by I_{Ln} and V_{Sn}. The special implementation condition of CIPF is that $Z_{3n} + Z_{fn} = 0$ and $K_n >> k_{31}(Z_{1n} + Z_{Sn})$. All the harmonic currents generated by the nonlinear power load will flow into the filtering branches, only if we guarantee that $Z_{3n} + Z_{fn} = 0$. Hence, the impedance coordination between the filtering branches and filtering winding is required. The function of K_n is to prevent the background harmonic from flowing into the filtering branches via the grid winding, and to help the harmonic currents generated by the nonlinear load sink into the filtering branches. The harmonic currents at the grid side can be totally filtered out in this way.

III. Control Strategy

Fig. 3 gives the comprehensive control system of the VICC strategy. This system consists of three parts:

1) one for extracting the grid-side harmonic currents to dampen the harmonic resonance;
2) one for extracting the harmonic components from the filtering branch currents to realize the zero-impedance design;
3) one for extracting the active component from the dc voltage to regulate the dc voltage of VSI. The control objective is to control the inverter's output voltage to satisfy the control law (1).

A. Harmonic Damping Control

There are plenty of existing literatures introducing the harmonic detection method. For instance, literature [17] uses a so-called *p–q* theory in the synchronous reference frames (*d–q* coordinates) to transform the currents. And, the stationary reference frames (*abc* to α–β) is applied to the resonant compensator [18]. The conventional harmonic detection algorithm is to calculate the fundamental component, and then subtracts it from the sampled grid-side current. The controlled quantity includes all the harmonic components except the fundamental components [19]. However, in practice, due to the nonlinearity of the system's components, the zero sequence harmonic may be generated at the grid side when the system shown in Fig. 1 is in operation. There is no flow path in the filtering branches, and the control strategy increase the harmonic components at the grid side, which means that the content of zero sequence harmonic will be greatly increased. Hence, unlike aforementioned studies, the proposed harmonic damping control adopts the fractional frequency detection method to adjust the degree of compensation of each order harmonic, and the main order harmonic components, i.e., 5th-, 7th-, 11th-, and 13th-order, are considered. The harmonic damping coefficient K_n acts as a zero impedance at the unconsidered frequency, such as the fundamental frequency, and as a damping resistor at the specific frequency to damp harmonic between Z_{Sn} and Z_{1n}. It should be remarked that the proposed harmonic damping control is an auxiliary contribution of the proposed control strategy.

When considering the system transfer function, the load current or the grid-side voltage (I_{Ln} or V_{Sn}) is regarded as the input of the control system, the grid-side current (I_{Sn}) as the output and the ac port voltage of VSI (V_C) as the feedback, one can obtained that

$$I_{Sn} = A(s)(-I_{Ln}) - C(s)V_C \tag{3}$$

$$I_{Sn} = B(s)(V_{Sn}) - C(s)V_C. \tag{4}$$

In Fig. 4(a), $H(s)$ is a low-pass filter (LPF) used in the process of harmonic detection, and

$$\begin{cases} A(s) = \dfrac{k_{21}(Z_{1n} + Z_{Sn})}{(Z_{3n} + Z_{fn}) + k_{31}^2(Z_{1n} + Z_{Sn})} \\ B(s) = \dfrac{k_{31}^2}{(Z_{3n} + Z_{fn}) + k_{31}^2(Z_{1n} + Z_{Sn})} \\ C(s) = \dfrac{k_{31}}{(Z_{3n} + Z_{fn}) + k_{31}^2(Z_{1n} + Z_{Sn})} \\ H(s) = \dfrac{\omega_C}{1 + \omega_C}. \end{cases} \tag{5}$$

According to (3), (4), and the system parameters given in Tables I and II in Section IV, the closed-loop model of the proposed CIPF system shown in Fig. 4(a) and the bode plots shown in Fig. 4(b) and (c) are obtained to investigate the harmonic

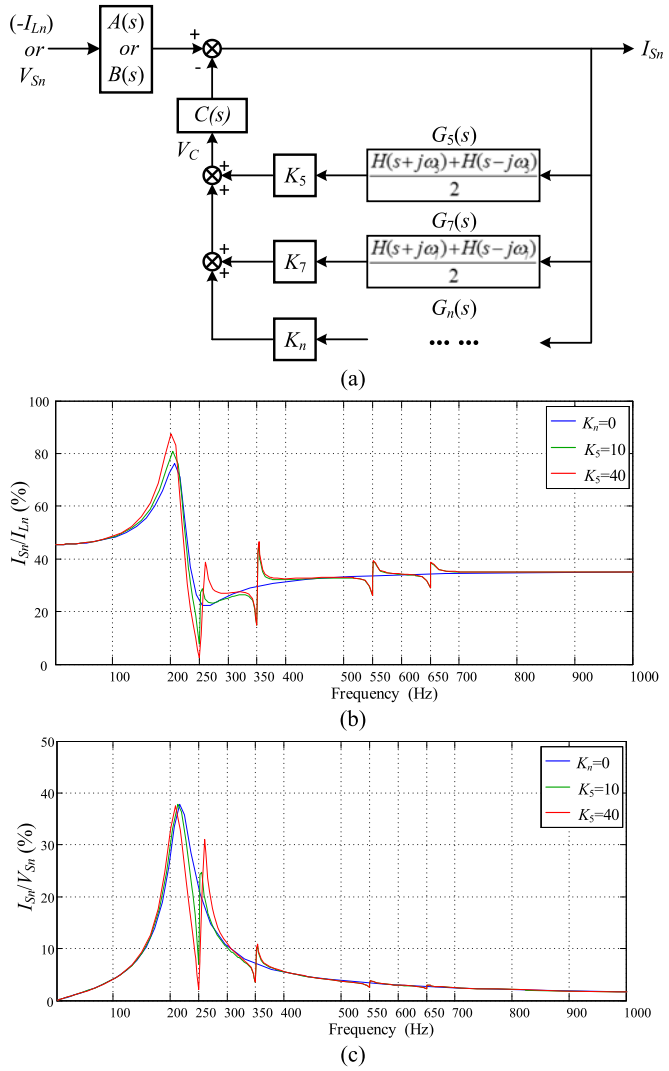

Fig. 4. Closed loop of the CIPF control system and the harmonic damping characteristics of the harmonic damping control method. (a) Closed loop of the CIPF control system; (b) considering I_{Sn}/I_{Ln}; (c) considering I_{Sn}/V_{Sn}.

TABLE I
PARAMETERS OF THE FT BRANCHES

Capacitance C_{f5} (μF)	248
Inductance L_{f5} (mH)	1.668
Q	1.048

damping characteristics [20]. Note that the bode plots mainly concern about the impact of different fifth harmonic damping control coefficient K_5 on the filtering performance, and the line resistance has been taken into account.

It can be found from Fig. 4(b) that the traditional PPF-based IPF method (i.e., $K_n = 0$) can only eliminate the harmonic around the tuning point ($f = 250$ Hz), and the filtering performance is inevitably affected by the line resistance. When the frequency is higher than 500 Hz, the frequency characteristic curve become a horizontal line, which means that for the higher-order harmonic beyond the tuned point, the IPF method cannot work effectively. After implementing the harmonic damping control

TABLE II
PARAMETERS OF THE IFRT

	Grid winding	Valve winding	Filtering winding
Wiring mode	Star	Star	Delta
Phase voltage (V)	230.94	100.00	57.70
Capacity (kVA)	30	30	20
Equivalent impedance (%)	5.27	−0.29	3.76

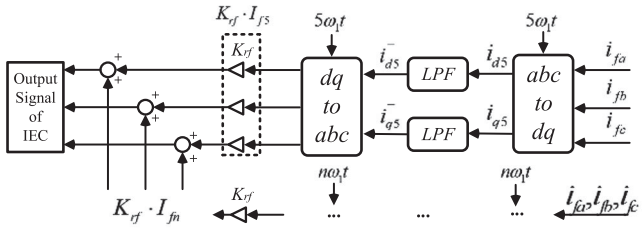

Fig. 5. Control algorithm of the IEC.

with the fractional frequency detection method ($K_5 = 10$ or $K_5 = 40$, and $K_7 = K_{11} = K_{13} = 20$), not only the main characteristic harmonic ($f = 250$, 350, 550, and 650 HZ) can be eliminated accurately, and it shows a lower impedance around these frequencies, but also the filtering frequency band for the considered order harmonic is increased. Moreover, the filtering performance gets better with the increase of K_n. But in practice, an excessive K_n is counter-productive, and the system stability may get worse. As shown in Fig. 4(c), when the CIPF system is not implemented ($K_n = 0$), the filtering system is completely powerless to suppress the main background harmonic frequency [$f = 250$ and 350 Hz, measured data can be found in Fig. 12(c)]. All the background harmonic components will flow into the grid winding of the IFRT without any blocking. Similarly, the curve maintains at a low level around the main order harmonic frequencies ($f = 250$, 350, 550, and 650 HZ) after the implementation of the control strategy. In other word, the harmonic resonance is hardly excited around these frequencies.

B. Zero-Impedance Control

The aim of zero-impedance control is to make the sum of the impedance of the filtering winding and the filtering branches to be zero, so that the essential condition for implementing CIPF can be satisfied. It is composed of two parts: 1) IEC with the design concept to cancel the resistance existed in the filtering winding and filtering branches, and adjust the Q of the passive power device; 2) MTC with the design concept to ensure the LC resonance at the considered harmonic frequency.

1) Impurity-Elimination Control: Figs. 5 and 6 present the control algorithm of IEC and its circuit model, respectively. Three-phase currents of the filtering branches are first sampled online. Then, by means of the instantaneous reactive power theory [19], the fifth-order harmonic component existed in the current flowing into the passive power device can be calculated. The fifth-order harmonic current is multiplied by the corresponding control coefficient, and the output signal of the IEC can be obtained.

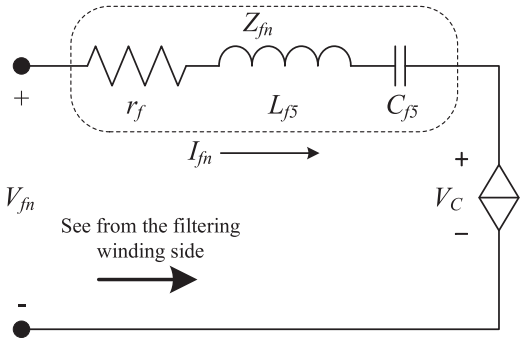

Fig. 6. Single-phase equivalent circuit of the filtering branches.

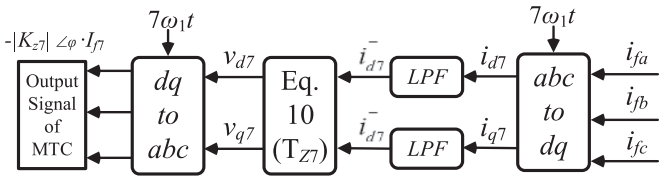

Fig. 7. Control algorithm of the MTC.

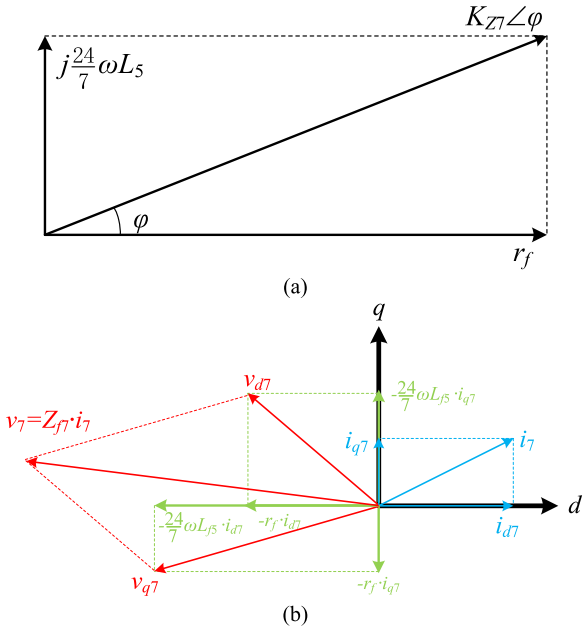

Fig. 8. Phasor relationship diagram. (a) Impedance of the filtering branches; (b) *dq* transformation.

As shown in Fig. 6, at the fifth-order harmonic frequency, when seeing from the filtering winding, the voltage of the filtering branches can be expressed as

$$V_{f5} = \underbrace{(j\omega_5 L_{f5} - j\frac{1}{\omega_5 C_{f5}} + r_f)}_{Z_{f5}} \cdot I_{f5} + \underbrace{K_{R5} \cdot I_{f5}}_{V_C}. \quad (6)$$

Assuming that the single-tuned filter has been well tuned at the fifth-order harmonic frequency, the voltage can be further simplified to

$$V_{f5} = \underbrace{(r_f + K_{R5})}_{Z_{f5}} I_{f5}. \quad (7)$$

If the IEC coefficient K_{R5} is controlled to be equal to $-r_f$, the voltage of the filtering branches is 0, which means that the total impedance of the filtering branches is 0. Hence, the internal resistance of the filtering branches can be eliminated. Besides, the Q of the single-tuned filter tends to be infinity, and the frequency selectivity will be better. In the bode plots, which show the harmonic damping characteristics [see Fig. 4(b) and (c)], the curve will be lower around the fifth-order harmonic frequency. Here, K_{R5} can be considered as a virtual negative resistance connected with the filtering branches in series. In addition, K_{R5} can be adjusted properly as needed to reach the design value of Q, and a satisfactory harmonic blocking performance can be realized.

2) Multituned Control: Figs. 7 and 8 give the control algorithm of MTC and the related phasor relationship, respectively. Similarly, with the IEC method, its detection algorithm calculates the seventh-order harmonic component existed in the filtering branch current, and the *dq* transformation is used. As shown in Fig. 6 and Fig. 8(a), at the seventh-order harmonic frequency, the relationship of the filtering branches is given by

$$\begin{cases} Z_{f7} = j7\omega L_{f5} - j\dfrac{1}{7\omega C_{f5}} + r_f \\ 5\omega = \dfrac{1}{\sqrt{L_{f5}C_{f5}}}. \end{cases} \quad (8)$$

Equation (8) can be further simplified, and the total impedance of the filtering branch is obtained, that is

$$Z_{f7} = r_f + j\frac{24}{7}\omega L_{f5} = |K_{Z7}|\angle\varphi. \quad (9)$$

The control algorithm is described as follows. As shown in Fig. 7, after the *dq* transformation, the three-phase filtering branches currents (i_{fa}, i_{fb}, i_{fc}) can be transformed into to two dc components $(\bar{i}_{d7}, \bar{i}_{d7})$ in *d–q* coordinates, by means of a LPF. Then, the reference voltage of the MTC control can be obtained by multiplying an impedance matrix T_{Z7} in (10). At last, the output signal of the MTC is calculated by the inverse *dq* transformation. The output voltage of the VSI will be $-|K_{z7}|\angle\varphi\cdot I_{f7}(Z_{f7} = |K_{z7}|\angle\varphi)$.

$$\begin{bmatrix} v_{d7} \\ v_{q7} \end{bmatrix} = \underbrace{\begin{bmatrix} -r_f & \frac{24}{7}\omega L_{f5} \\ -\frac{24}{7}\omega L_{f5} & -r_f \end{bmatrix}}_{T_{Z7}} \begin{bmatrix} \bar{i}_{d7} \\ \bar{i}_{q7} \end{bmatrix}. \quad (10)$$

By the MTC method, the VSI can be equivalent to a virtual negative impedance connected with the filtering branches in series, and the virtual impedance is capacitive at seventh-order harmonic frequency, which makes the total impedance of the filtering be 0. By means of a set of single-tuned filter, the objective of mutlituned can be realized.

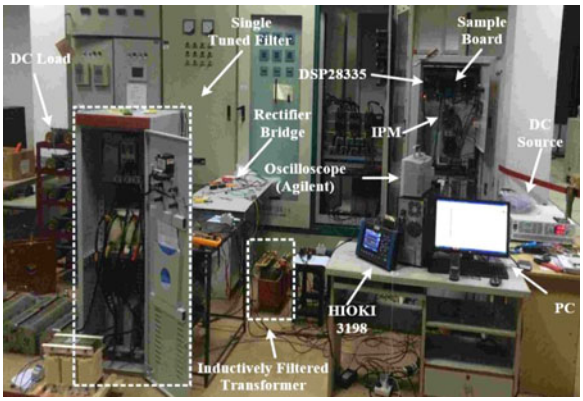

Fig. 9. Prototype of the CIPF system.

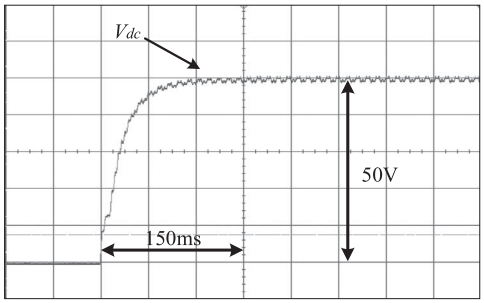

Fig. 10. Transient waveform of the dc voltage (recorded by Agilent).

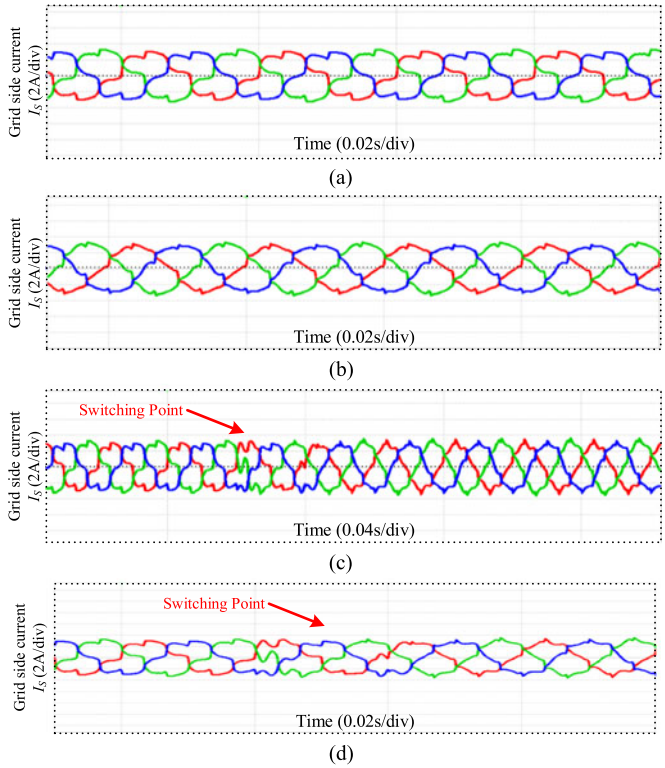

Fig. 11. Experimental results about the grid side current I_S of the VICC-based CIPF (recorded by HIOKI). (a) Waveform of I_{Sn} when implementing IPF method; (b) waveform of I_{Sn} when implementing VICC-based CIPF; (c) transient waveform when switching the VSI; (d) detailed waveform when switching the VSI.

IV. Experiment Verification

In order to validate the proposed VICC strategy, a 5-kVA prototype of the CIPF system in the laboratory is established, as shown in Fig. 9. The dc voltage of the VSI is 50 V, and the dc capacitance is 1.5 μF. A DSP (TMS320F28335) is chosen as the main control chip with a carrier frequency of 10 kHZ for implementing the VICC strategy in this system. The design parameters of the FT branches and the IFRT are listed in Tables I and II, respectively. A HIOKI-PW3198 PQ analyzer and an Agilent DSO-X 3024 are used to record the voltage and the current data. The experimental results are shown in Figs. 10–12.

As shown in Fig. 10, the fluctuated range of the dc voltage is within 5% of the reference value (50 V) after a setting time of 150 ms, by means of the regulation of the dc voltage control. The capacitor is not precharged, and its initial voltage is 0. The public grid is used in the laboratory to provide the power supply, and the total harmonic distortion (THD) of the grid voltage is 1.78%. Besides, it can be observed from Figs. 11(a) and 12(c) that the existence of the background harmonic voltage seriously affects the filtering performance of the IPF system. The contents of the fifth- and the seventh-order harmonic components in the grid-side current I_{Sn} are increased. However, after the implementation of the harmonic damping control and the zero-impedance control, as shown in Fig. 11(b) and Fig. 12(b), the harmonic components are greatly decreased, and the $\mathrm{THD_{IS}}$ is reduced from 21.48% to 9.34%. The current waveform represents a good sinusoid. Further, from the experimental results shown in Fig. 11(c) and (d), it can be found that the proposed system shows a good dynamic and steady performance.

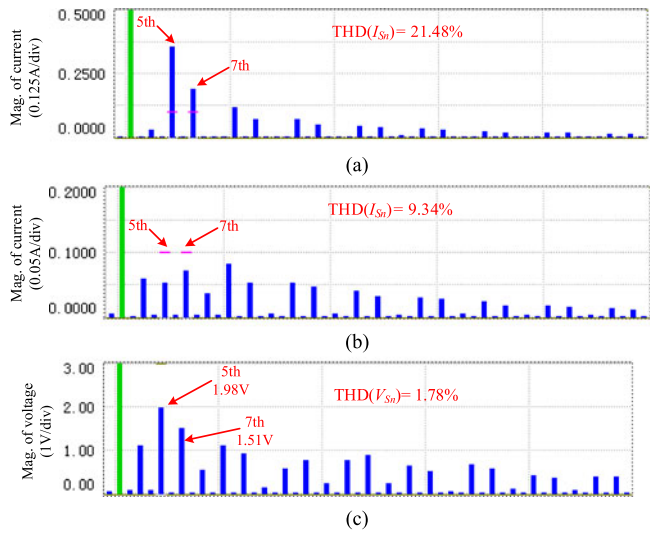

Fig. 12. Harmonic spectra of the current at the grid side of the IFRT and the voltage of the public grid. (a) With IPF method; (b) with VICC-based CIPF; (c) background harmonic voltage of the public grid used in the laboratory.

V. Conclusion

This letter proposes a VICC strategy for the CIPF system. Two solutions are presented aiming to weaken the influence of background harmonic voltage and realize the zero-impedance design of CIPF, that is, the harmonic damping control and the zero-impedance control. The harmonic components generated by the background harmonic voltage of the distribution network can be eliminated effectively around the specific harmonic frequency. Moreover, by the virtual impedance control, the Q of the power passive device can be adjusted, and a virtual single-tuned LC filter is created at the considered harmonic frequency. At last, the experimental results validate the proposed VICC-based CIPF system.

References

[1] D. Detjen, J. Jacobs, R. W. De Doncker, and H. G. Mall, "A new hybrid filter to dampen resonances and compensate harmonic currents in industrial power systems with power factor correction equipment," *IEEE Trans. Power Electron.*, vol. 16, no. 6, pp. 821–827, Nov. 2001.

[2] J. Phinney and D. J. Perreault, "Filters with active tuning for power applications," *IEEE Trans. Power Electron.*, vol. 18, no. 2, pp. 636–647, Mar. 2003.

[3] D. A. Gonzalez and J. C. McCall, "Design of filters to reduce harmonic distortion in industrial power systems," *IEEE Trans. Ind. Appl.*, vol. IA-23, no. 3, pp. 504–511, Apr. 2008.

[4] D. Li, K. Yang, Z. Q. Zhu, and Y. Qin, "A novel series power quality controller with reduced passive power filter," *IEEE Trans. Ind. Electron*, 2016.

[5] Y. Chen, "Optimal multi-objective single-tuned harmonic filter planning," *IEEE Trans. Power Del.*, vol. 20, no. 2, pp. 1191–1197, Apr. 2005.

[6] H. Fujita, T. Yamasaki, and H. Akagi, "A hybrid active filter for damping of harmonic resonance in industrial power systems," *IEEE Trans. Power Electron.*, vol. 15, no. 2, pp. 215–222, Mar. 2000.

[7] H. Akagi and K. Isozaki, "A hybrid active filter for a three-phase 12-pulse diode rectifier used as the front end of a medium-voltage motor drive," *IEEE Trans. Power Electron.*, vol. 27, no. 1, pp. 69–77, Jan. 2012.

[8] H. Akagi and R. Kondo, "A transformerless hybrid active filter using a three-level pulsewidth modulation (PWM) converter for a medium-voltage motor drive," *IEEE Trans. Power Electron.*, vol. 25, no. 6, pp. 1365–1374, Jun. 2010.

[9] Y. Li, L. Lou, C. Rehtanz, S. Ruberg, D. Yang, and J. Xu, "An industrial DC power supply system based on an inductive filtering method," *IEEE Trans. Ind. Electron.*, vol. 59, no. 2, pp. 714–722, Feb. 2012.

[10] Y. Li, L. Luo, C. Rehtanz, D. Yang, S. Rüberg, and F. Liu, "Harmonic transfer characteristics of a new HVDC system based on an inductive filtering method," *IEEE Trans. Power Electron.*, vol. 5, no. 5, pp. 2273–2283, May 2012.

[11] S. Hu *et al.*, "A new integrated hybrid power quality control system for electrical railway," *IEEE Trans. Ind. Electron.*, vol. 62, no. 10, pp. 6222–6232, Oct. 2015.

[12] Y. Li, F. Liu, T. K. Saha, O. Krause, and Y. Cao, "Hybrid inductive and active filtering method for damping harmonic resonance in distribution network with non-linear loads," *IET Power Electron*., vol. 8, no. 9, pp. 1616–1624, Sep. 2015.

[13] C. Liang *et al.*, "An integrated harmonic-filtering transformer for low-voltage distribution systems," *IEEE Trans. Magn.*, vol. 51, no. 11, Nov, 2015, Art. no. 8402204.

[14] Y. Li, T. K. Saha, O. Krause, Y. Cao, and C. Rehtanz, "An inductively active filtering method for power-quality improvement of distribution networks with nonlinear loads," *IEEE Trans. Power Del.*, vol. 28, no. 4, pp. 2465–2473, Oct. 2013.

[15] X. Wang, Y. W. Li, F. Blaabjery, and P. Chiang Loh, "Virtual-impedance-based control for voltage-source and current-source converters," *IEEE Trans. Power Electron.*, vol. 30, no. 12, pp. 7019–7037, Dec. 2015.

[16] M. J. Heathcote, *The J&P Transformer Book*, 12th ed. Oxford, U.K.: Reed Educ. Prof. Publ. Ltd., 1998.

[17] R. Inzunza and H. Agagi, "A 6.6-kV transformerless shunt hybrid active filter for installation on a power distribution system," *IEEE Trans. Power Electron.*, vol. 20, no. 4, pp. 893–900, Jul. 2005.

[18] W. Lenwari, M. Sumner, and P. Zanchetta, "The use of genetic algorithms for the design of resonant compensators for active filters," *IEEE Trans. Ind. Electron.*, vol. 56, no. 8, pp. 2852–2861, Aug. 2009.

[19] H. Akagi, E. H. Watanabe, and M. Aredes, *Instantaneous Power Theory and Applications to Power Conditioning*. Hoboken, NJ, USA: Wiley, 2007.

[20] R. S. Burns, *Advanced Control Engineering*. Oxford, U.K.: Butterworth-Heinemann, 2001.